

Supplemental Fig. 1 The *C. elegans* calcineurin B homolog, *cnb-1*, regulates TDP-43 phosphorylation *in vivo*. (a) A loss of function mutation in the calcineurin regulatory subunit *cnb-1* increases phosphorylation and total protein levels of WT TDP-43 transgenic *C. elegans*. (b) Bar graphs represent measurement of 3 independent replicate immunoblots. Significance was evaluated using Student's t-test between TDP-43(WT) and TDP-43(WT); *cnb-1(jh103)*. $p=0.04$ comparing pTDP band intensities. $p=0.04$ comparing total TDP-43 band intensities. (c) *cnb-1* loss of function increases pTDP and total TDP in M337V TDP-43 transgenic *C. elegans*. (d) Bar graphs are quantitation of 3 independent replicate immunoblots. Significance was evaluated using Student's t-test between TDP-43(M337V) and TDP-43(M337V); *cnb-1(jh103)*, $p=0.001$ comparing pTDP band intensities. $p=0.003$ comparing total TDP-43 band intensities. (e) TDP-43(M337V) and TDP-43(M337V); *cnb-1(jh1035)* were subjected to sequential protein extraction with detergents of increasing solubilizing strengths. Levels of sarkosyl-insoluble (SARK) pTDP are increased with loss of *cnb-1*. (f) Dispersal velocities of normal and mutant control worm strains were measured by calculating the radial distance traveled from a designated central starting point over 30 minutes. $N>100$ for each genotype tested. *cnb-1(jh103)* is significantly hyperactive relative to wild-type worms, $p<0.01$. (g) TDP-43(M337V); *cnb-1(jh103)* animals have significantly reduced locomotion velocity compared to TDP-43(M337V) alone. $N>130$ per genotype, $p=0.01$. (c) TDP-43(M337V SS/AA); *cnb-1(jh103)* move better than TDP-43(M337V SS/AA) alone, comparable to the *cnb-1(jh103)* hyperactivity observed in (f). $N>200$, $p<0.001$.

Supplemental Fig. 2 *C. elegans* TDP-43 tg; *tax-6(-)* animals exhibit nerve cord defasciculation and GFP foci. (a-c) High-magnification images of identical posterior segments of the ventral nerve cord and axonal processes. (a) *tax-6(ok2065)* have normal fasciculation of axonal bundles and commissures that extend from the dorsal to the ventral nerve cord. (b) TDP-43(A315T) have nodes of higher-intensity GFP-positive foci and lose axonal commissures between the dorsal and ventral nerve cords. (c) TDP-43(A315T); *tax-6(ok2065)* have nodes of higher-intensity GFP-positive foci, loss of axonal processes, and exhibit axonal defasciculation. (d) High-magnification image of a

segment of the TDP-43(A315T); *tax-6(ok2065)* ventral nerve cord near the vulva. TDP-43(A315T); *tax-6(ok2065)* display severe axonal defasciculation, dystrophic neurites, and nodes of higher-intensity GFP-positive foci.

Supplemental Fig. 3 Calcineurin inhibition and activation have opposite effects on pTDP. (a) HEK293 cells treated with the calcineurin inhibitor FK506 accumulate pTDP-35. (b) HEK293 cells treated with NiCl₂ have reduced pTDP-35. (c) HDAC6 mRNA levels do not significantly change in response to FK506 or ethacrynic acid. Expression levels of HDAC6 were tested by quantitative reverse transcription PCR (qRT-PCR). Three independent experiments were evaluated and combined for the average relative expression change. All values were normalized to the housekeeping gene GAPDH. Error bars are standard deviation. Significance was evaluated using one-way analysis of variance with Tukey's multiple comparison test, but no significant differences were found between experimental conditions. (d) Splicing of TDP-43 regulated genes FNIP, POLDIP3/SKAR, and STAG2 was evaluated using RT-PCR. Relative intensities of mRNA splice isoforms were unchanged between experimental samples.

Supplementary Fig. 4 Calcineurin co-localizes with pTDP pathology in FTLD-TDP hippocampus. (a) 60X fluorescent panel image of DAPI (Blue), calcineurin (Green), pTDP (Red). (b) Colocalization of calcineurin and pTDP. (c) Plot of pTDP and calcineurin colocalization (Pearson's coefficient of correlation = 0.5502). (d) DAPI. (e) Calcineurin. Peripheral 50µM or larger filamentous bodies observed here and in (a-b) are green autofluorescent artifacts from tissue preparation (See Supplementary Fig. 6 for single label calcineurin immunostaining). (f) pTDP.

Supplementary Fig. 5 Calcineurin co-localizes with pTDP pathology in FTLD-TDP frontal cortex. (a) 60x fluorescent panel image of DAPI (Blue), calcineurin (Green), pTDP (Red). (b) Colocalization of calcineurin and pTDP. (c) Plot of pTDP and calcineurin colocalization (Pearson's coefficient of correlation = 0.6433). (d) DAPI. (e) Calcineurin. (f) pTDP.

Supplemental Fig. 6 Single label calcineurin immunofluorescence immunostaining is consistent with double label immunostaining data from Supplemental Figs. 4 and 5. Immunostaining in FTLD-TDP hippocampus (a) calcineurin, (b) DAPI, (c) merge image, and in FTLD-TDP frontal cortex (d) Calcineurin, (e) DAPI, and (f) merge image.

Supplemental Fig. 7 Calcineurin co-localizes with pTDP pathology in ALS spinal cord motor neurons. Immunofluorescence of (a) DAPI, (b) calcineurin, (c) pTDP. (d) Merge image of DAPI, calcineurin, and pTDP immunofluorescence. (e) Colocalization of calcineurin and pTDP. (f) Plot of pTDP and calcineurin colocalization (Pearson's coefficient of correlation = 0.8785).

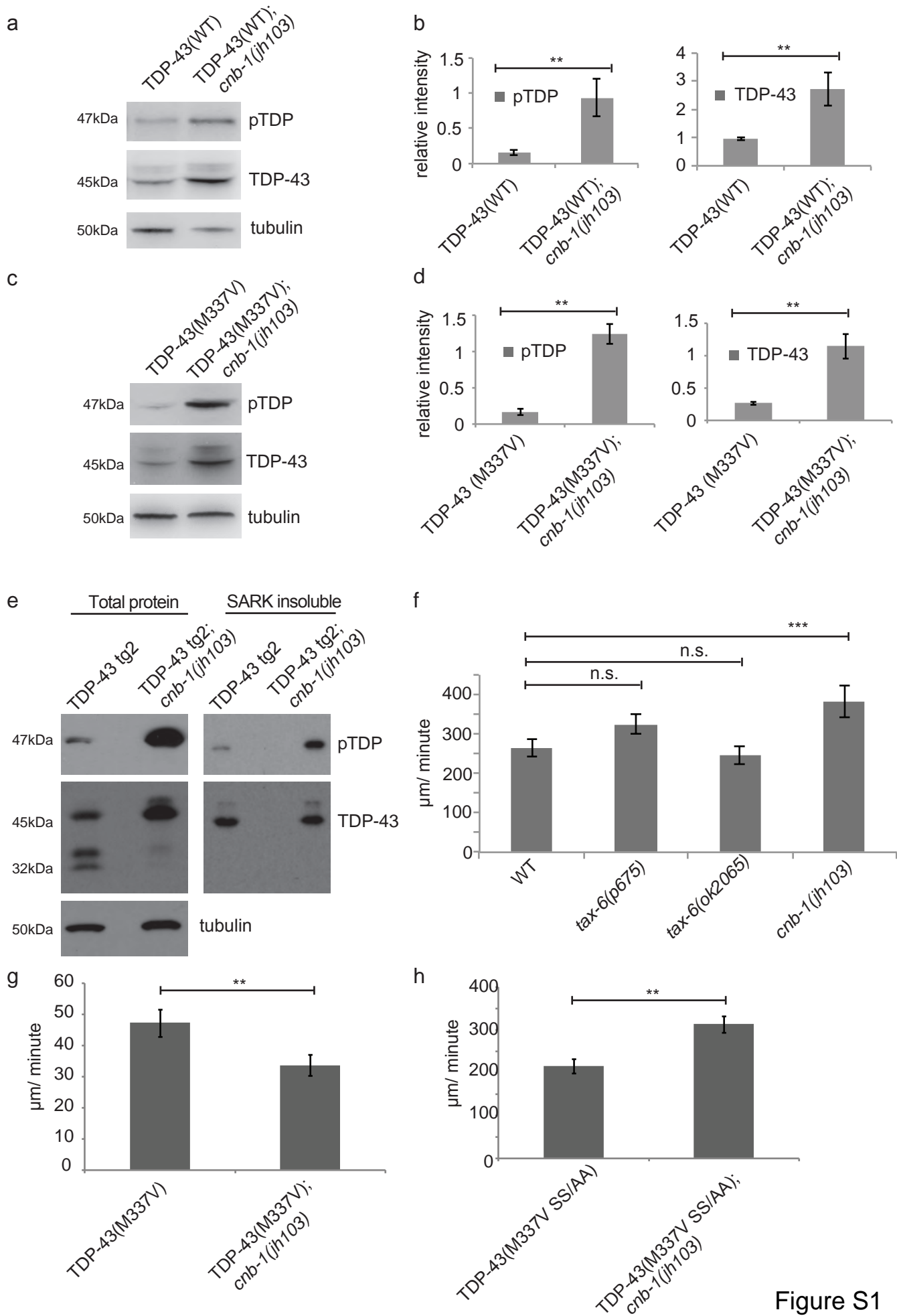


Figure S1

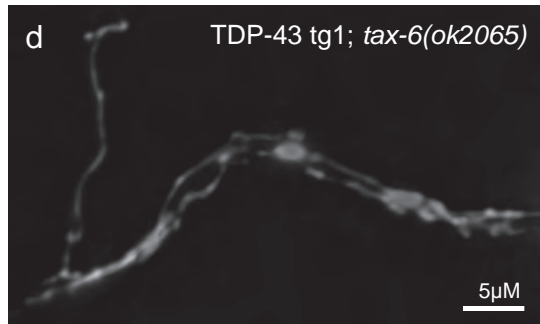
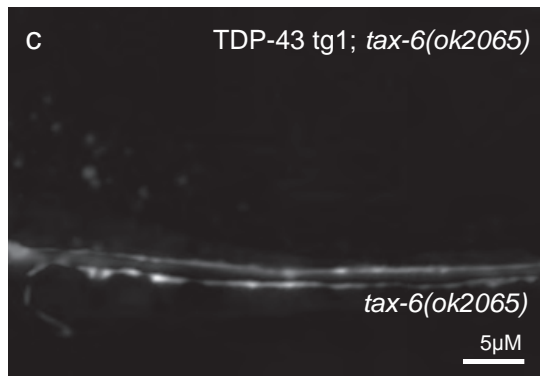
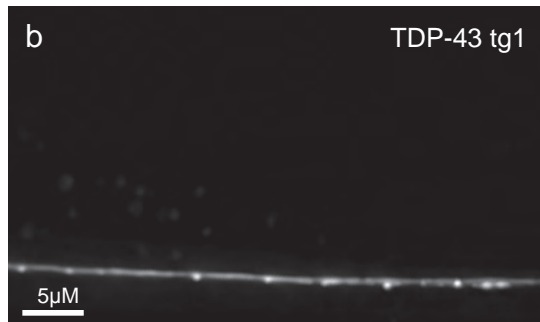
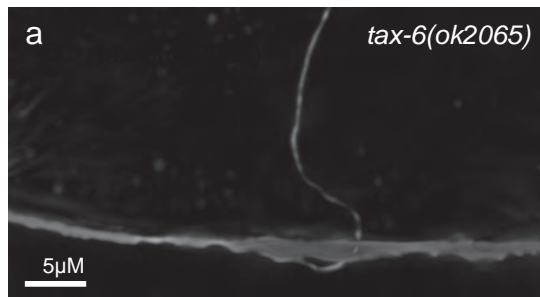


Figure S2

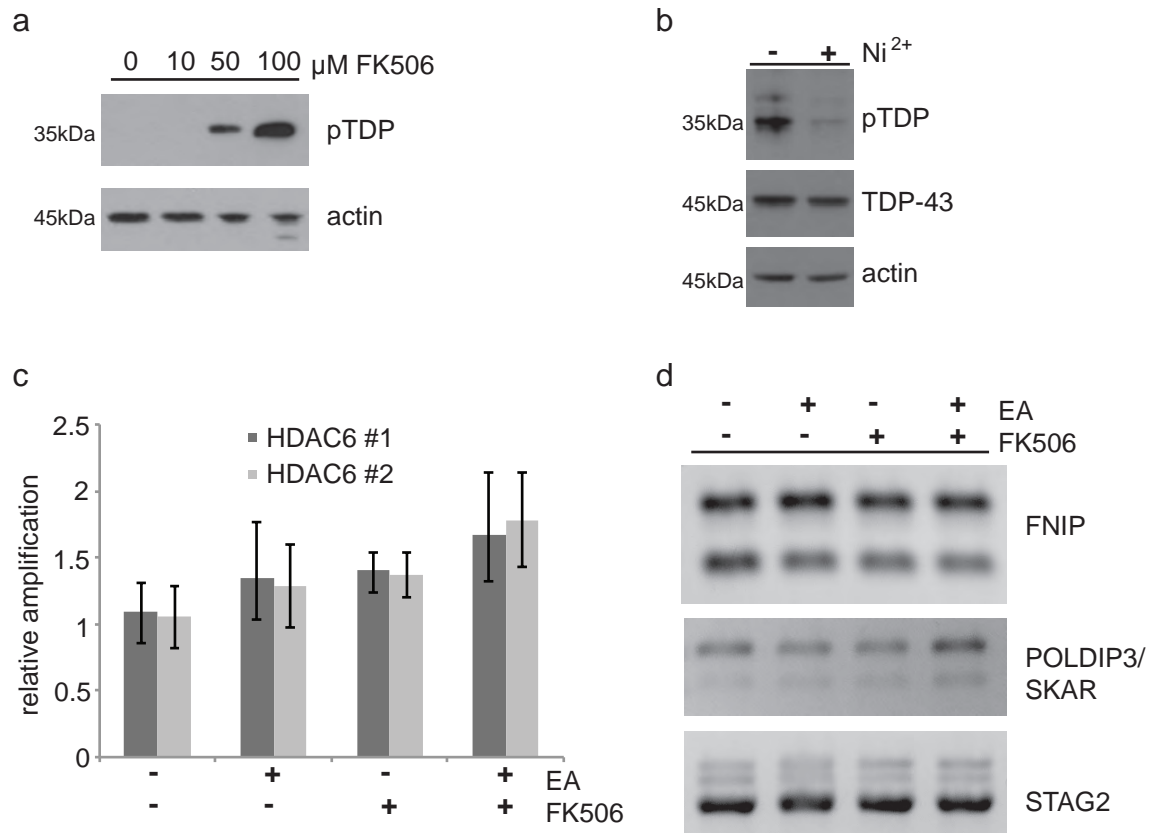


Figure S3

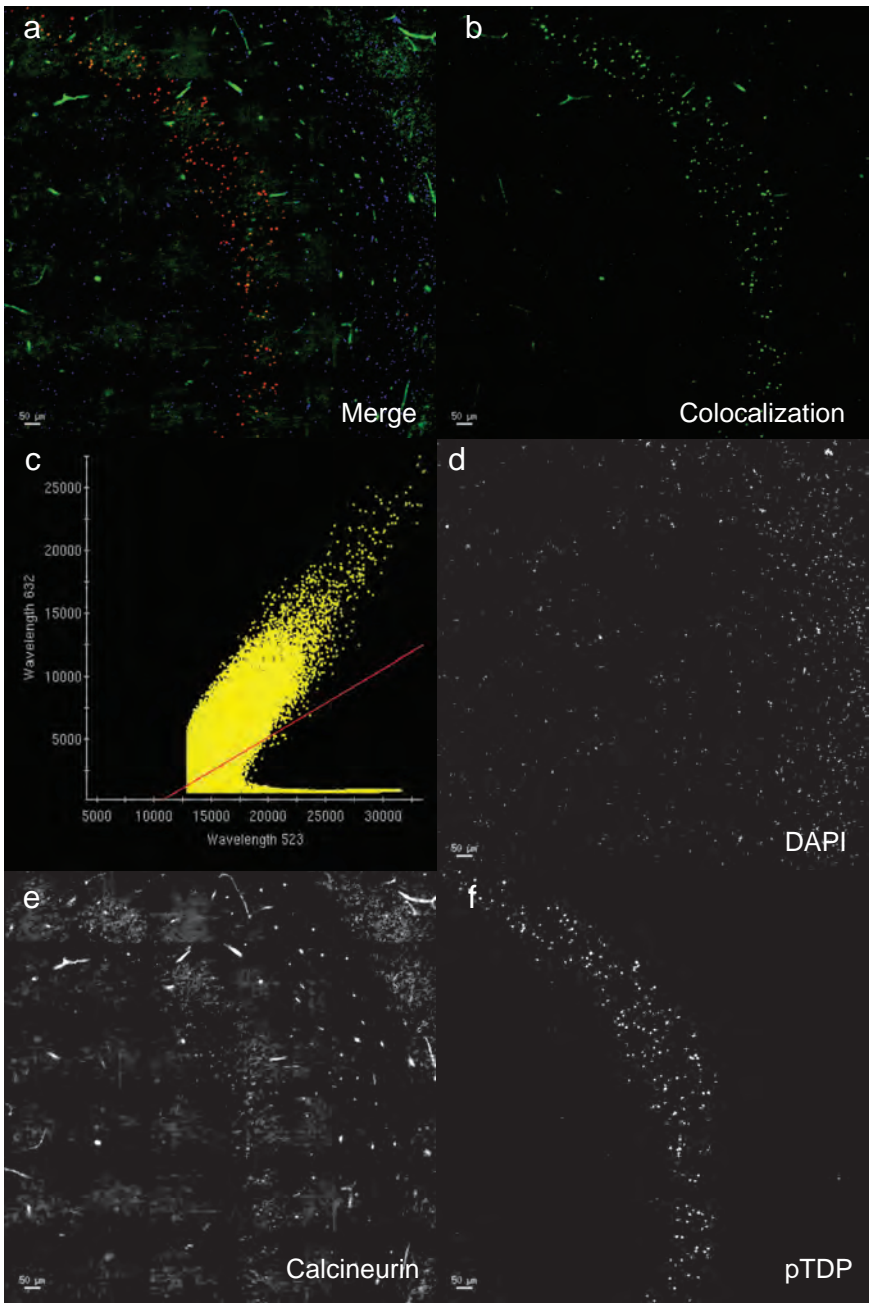


Figure S4

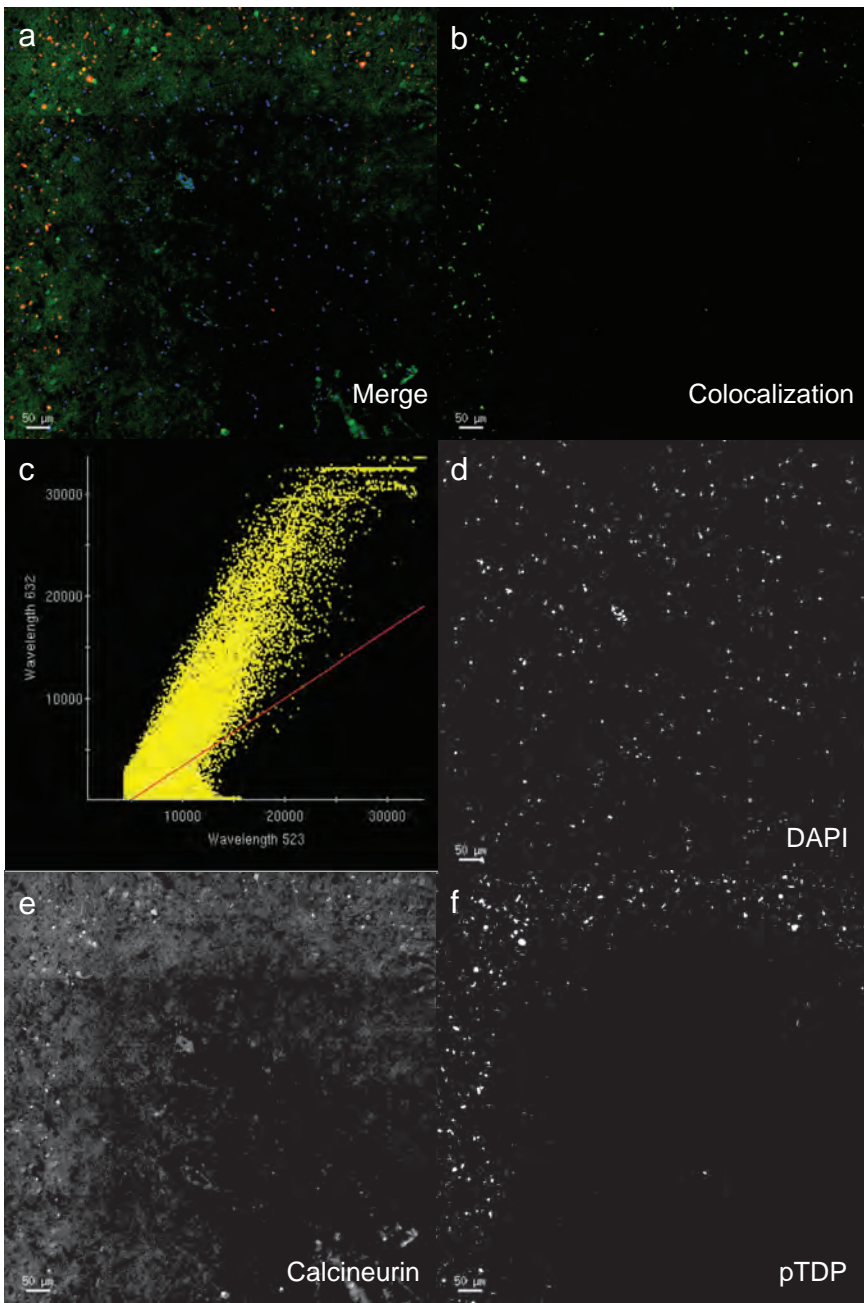


Figure S5

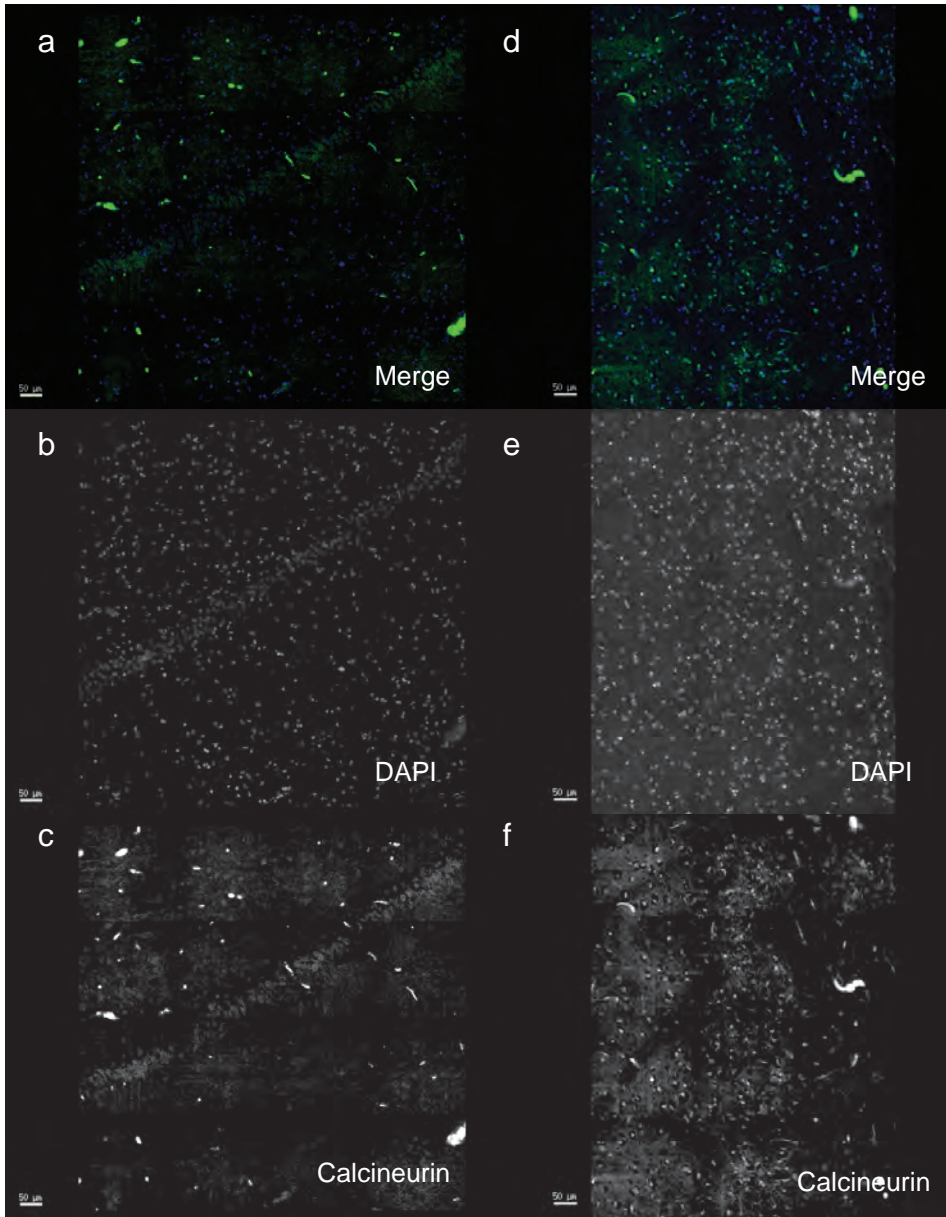


Figure S6

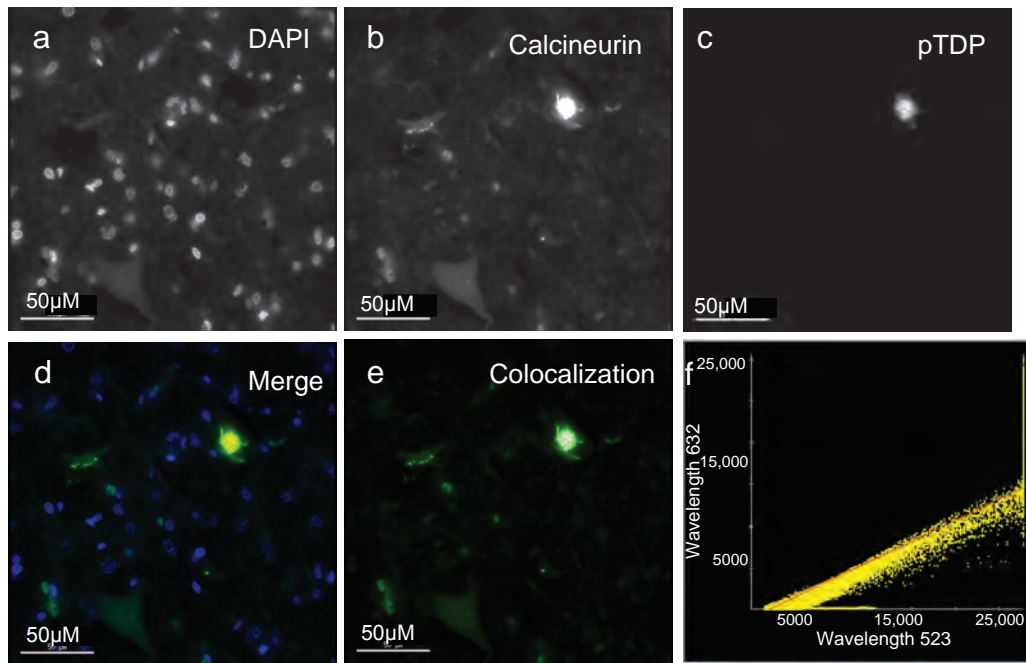


Figure S7